Volume 3 | Number 46 | 14 December 2015 | Pages 11977–12166

Journal of Materials Chemistry C

Materials for optical, magnetic and electronic devices

www.rsc.org/MaterialsC

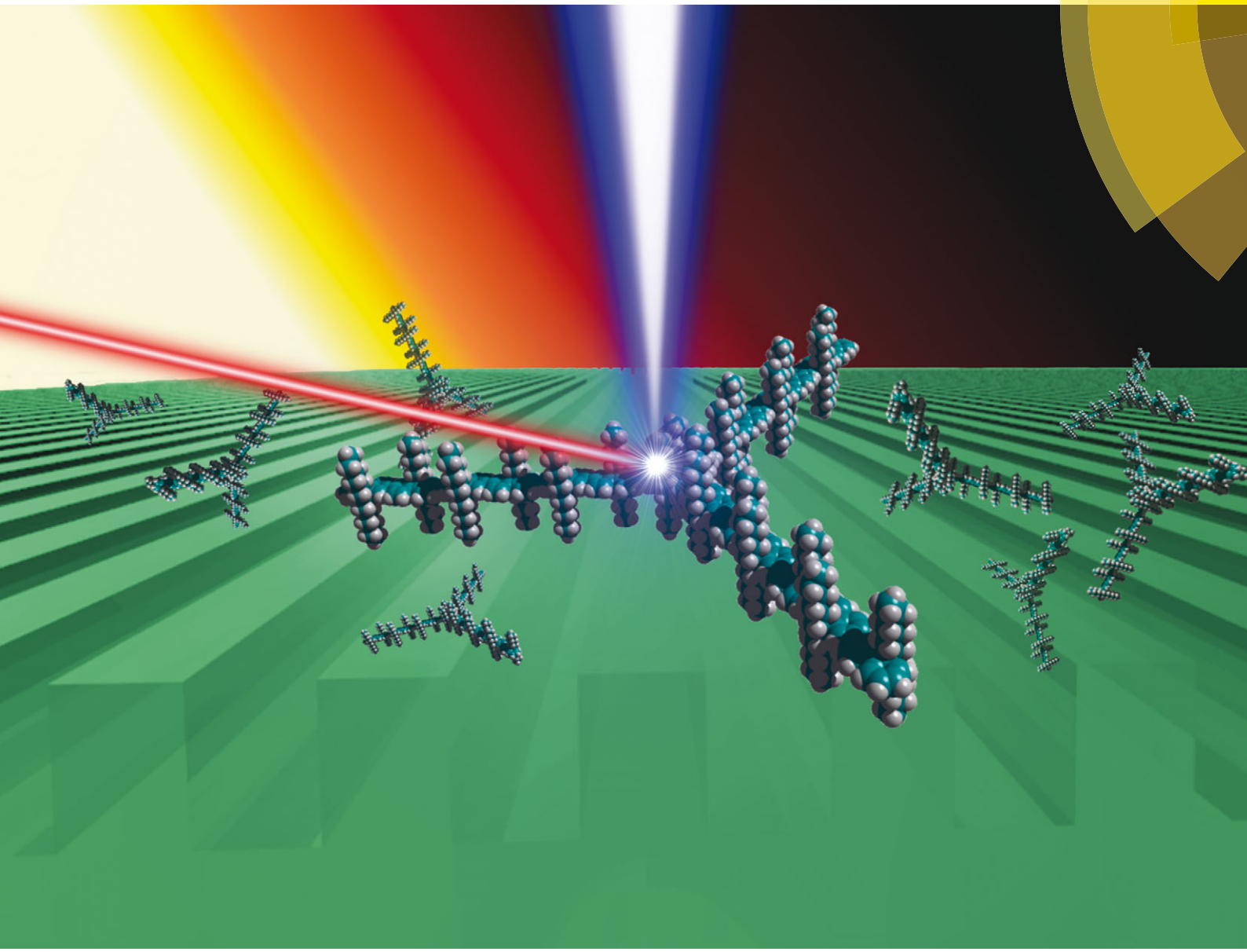

ISSN 2050-7526

ROYAL SOCIETY OF CHEMISTRY

PAPER

Peter J. Skabara, Hilmi Volkan Demir *et al.*

Ultralow-threshold up-converted lasing in oligofluorenes with tailored strong nonlinear absorption

Journal of Materials Chemistry C

PAPER

View Article Online
View Journal | View Issue

Cite this: J. Mater. Chem. C, 2015, 3, 12018

Ultralow-threshold up-converted lasing in oligofluorenes with tailored strong nonlinear absorption†

Burak Guzelturk,‡[a] Alexander L. Kanibolotsky,‡[bc] Clara Orofino-Pena,[b] Nicolas Laurand,[d] Martin D. Dawson,[d] Peter J. Skabara*[b] and Hilmi Volkan Demir*[ae]

Received 23rd July 2015,
Accepted 12th October 2015

DOI: 10.1039/c5tc02247a

www.rsc.org/MaterialsC

Nonlinear optical response in organic semiconductors has been an attractive property for many practical applications. For frequency up-converted lasers, to date, conjugated polymers, fluorescent dyes and small organic molecules have been proposed but their performances have been severely limited due to the difficulty in simultaneously achieving strong nonlinear optical response and high performance optical gain. In this work, we show that structurally designed truxene-based star-shaped oligofluorenes exhibit strong structure–property relationships enabling enhanced nonlinear optical response with favorable optical gain performance. As the number of fluorene repeat units in each arm is increased from 3 to 6, these molecules demonstrate a two-photon absorption cross-section as high as 2200 GM, which is comparable to that of linear conjugated polymers. Tailored truxene oligomers with six fluorene units in each arm (T6) show two-photon absorption pumped amplified spontaneous emission with a threshold as low as 2.43 mJ cm^{-2}, which is better than that of the lowest reported threshold in organic semiconductors. Furthermore, we show a frequency up-converted laser using the newly designed and synthesized star-shaped oligomer T6 with a threshold as low as 3.1 mJ cm^{-2}, which is more than an order of magnitude lower than that of any conjugated polymer. Thus, these oligomers with enhanced nonlinear optical properties are highly attractive for bio-integrated applications such as photodynamic therapy and *in vivo* bio-sensing.

Introduction

Over the past two decades, π-conjugated organic semiconductor materials have become promising as optical gain media toward functional organic lasers.[1–4] Among the π-conjugated materials, fluorescent star-shaped oligomers stand out thanks to their well-controlled dispersity and high uniformity.[5–7] These star-shaped oligomers offer favorable optical properties including high photoluminescence quantum yields in their solid-state films, where optical losses are also very small.[8] These advantageous properties together with ease of processing have already made such star-shaped oligomers appealing for various photonic applications including light-emitting diodes and single-photon absorption pumped lasers.[5,8–12]

Also, the nonlinear optical response in π-conjugated organic semiconductors attracts great interest in two-photon excited photoluminescence microscopy,[13–15] photodynamic therapy,[16] three-dimensional data storage,[17] microfabrication,[18] optical power limiting[19] and frequency up-converted lasing.[20–22] Previously, an enhanced two-photon absorption (2PA) cross-section has been demonstrated in structurally engineered oligomers[23–27] and molecules having elongated π-conjugation.[28,29] Yet, frequency up-converted lasers, which have attracted increasing scientific and technological interest,[30] have not been demonstrated in fluorescent oligomers except dendrimers,[31] conjugated polymers,[20,21] donor–acceptor type organic molecules[22,32] and various dyes.[30]

On the other hand, star-shaped oligomers have already shown outstanding optical gain performance under single-photon absorption (1PA) pumping accomplishing low lasing thresholds

[a] Department of Electrical and Electronics Engineering, Department of Physics, UNAM - Institute of Materials Science and Nanotechnology, Bilkent University, Ankara 06800, Turkey. E-mail: volkan@bilkent.edu.tr
[b] WestCHEM, Department of Pure and Applied Chemistry, University of Strathclyde, Thomas Graham Building, 295 Cathedral Street, Glasgow G1 1XL, UK. E-mail: peter.skabara@strath.ac.uk
[c] Institute of Physical-Organic Chemistry and Coal Chemistry, 02160 Kyiv, Ukraine
[d] Institute of Photonics, University of Strathclyde, Glasgow G4 0NW, UK
[e] Luminous! Center of Excellence for Semiconductor Lighting and Displays, School of Electrical and Electronic Engineering, School of Physical and Mathematical Sciences, Nanyang Technological University, Nanyang Avenue, Singapore 639798, Singapore. E-mail: hvdemir@ntu.edu.sg

† Electronic supplementary information (ESI) available. See DOI: 10.1039/c5tc02247a

‡ These authors contributed equally to this work.

with ultra-large bandwidth spectral tunability in the deep-blue spectral region.[8,9,11,33,34] However, to date, these star-shaped oligomers have not been considered as two-photon absorption (2PA) pumped optical gain media, nor has their potential as frequency up-converted lasers.

Among star-shaped oligomers, the truxene core based molecules have shown high performance in several systems, which have demonstrated low lasing thresholds.[8,9] Moreover, truxenes are typically amorphous in nature,[35] which is ideal for their use in photonic applications that demand high quantum yields. In this respect, truxenes are superior to other cores, such as a simple benzene ring. For example, the truxene T4 has a lasing threshold of 270 W cm^{-2},[8] whereas the benzene analogue has a threshold of 1.2 kW cm^{-2}.[36]

In this work, we elucidate that truxene based star-shaped oligofluorenes have strong potential as a gain medium for frequency up-converted organic lasers since they provide simultaneously a large 2PA cross-section, substantially high photoluminescence quantum yields and large oscillator strengths. Truxene based star-shaped oligofluorenes have three conjugated arms, which consist of either three or four repeating fluorene units.[5] Here, we develop a new star-shaped oligofluorene (T6) having six repeating fluorene units in each fluorescent arm in an effort to maximize the nonlinear optical response in these oligomers. This design approach results in a large 2PA cross-section as high as 2200 GM. Then, we investigate the amplified spontaneous emission (ASE) under 2PA in these star-shaped oligomers. Newly synthesized T6 oligomers exhibit 2PA pumped ASE performance with an ultra-low threshold of 2.4 mJ cm^{-2} owing to the enhanced 2PA cross-section that is comparable to that of conjugated polymers.[20,29] Furthermore, we show the first frequency up-converted flexible distributed feedback (DFB) laser of star-shaped oligomers exhibiting a threshold as low as 3.1 mJ cm^{-2}, which outperforms the best reported organic semiconductor based frequency up-converted lasers.[20,21] Such NIR pumped up-converted organic lasers will be highly attractive for bio-integrated applications such as photodynamic therapy or *in vivo* bio-sensing.

Materials and methods

$Pd(PPh_3)_4$ was prepared according to the known procedure[37] and stored under nitrogen in a freezer. THF was purified using a solvent purification system SPS-400-5 Innovative Technology, Inc. All other reagents and solvents were purchased from commercial suppliers and used without further purification unless otherwise stated. ^1H and ^{13}C NMR spectra were recorded on a Bruker Avance DPX400 spectrometer at 400.1 and 100.6 MHz, respectively. Chemical shifts are given in ppm. MALDI mass spectrometry was performed on a Shimadzu Axima-CFR spectrometer. Thermogravimetric analysis (TGA) was conducted using a Perkin-Elmer Thermogravimetric Analyzer TGA7 under a constant flow of argon. Differential scanning calorimetry (DSC) was performed on a TA Instruments Q1000 equipped with a RC-90 refrigerated cooling unit attached.

Absorbance measurement was performed using a CARY 100 UV-Vis spectrometer. Solution-state photoluminescence was measured using a CARY Eclipse spectrometer. A femtosecond laser system consists of a Spectra Physics Tsunami mode-locked seed laser and a Spitfire Pro regenerative amplifier. We used Maya2000 (Ocean Optics) to collect the 1PA and 2PA pumped ASE and lasing spectra. We used a Newport Z-scan kit for the nonlinear absorption cross-section measurements.

Synthesis of the truxene based oligofluorene T6

To a degassed solution of **T2Br**[38] (302.5 mg, 98.24 μmol) and tetrakis(triphenylphosphine)-palladium(0) (37.5 mg, 32.5 μmol) in 10 mL of THF the boronic acid **F4B**[6,38] (700 mg, 509 μmol) was added, followed by $Ba(OH)_2{\cdot}8H_2O$ (305 mg, 967 μmol) and deionized water (0.64 mL). The mixture was degassed and heated to reflux for 20 hours. After cooling the mixture was quenched with brine and extracted with CH_2Cl_2. The combined extracts were dried over $MgSO_4$. After evaporation of the solvent the crude product was purified on a silica gel column eluting with a mixture of petroleum ether : CH_2Cl_2 1 : 10 ramping to 1 : 5, which afforded the product as a yellowish solid (585 mg, 85.8 μmol, 87%).

T6, MALDI-TOF MS: *m*/*z* 6836 ($(M + H)^+$), 6773 ($(M–C_6H_{14} + Na)^+$), 6752 ($(M–C_6H_{13})^+$); anal. calcd for $C_{513}H_{666}$: C, 90.18; H, 9.82%. Found: C, 90.21; H, 9.63%.

^1H NMR (400 MHz, δ, $CDCl_3$, see Fig. S1, ESI†): 8.53 (1H, bs), 8.10–7.50 (36H, m), 7.42–7.29 (3H, m), 3.11 (2H, bs), 2.65–1.75 (26H, m), 1.27–0.55 (154H, m).

^{13}C NMR ($CDCl_3$, δ, 100 MHz, see Fig. S2, ESI†) 153.97, 151.34, 151.00, 150.54, 140.32, 140.08, 139.86, 139.55, 125.68, 122.44, 121.06, 119.49, 119.23, 54.86, 54.69, 39.89, 31.09, 30.99, 29.20, 23.38, 22.11, 22.07, 21.87, 13.54, 13.45.

Results and discussion

The chemical structure of star-shaped oligofluorenes having varying fluorene arm lengths is presented in Fig. 1a. Depending on the number of repeating fluorene units in each arm, these molecules are called T3, T4 and T6. The T3 and T4 compounds were synthesized according to our previous reports.[6,38] The synthesis of T6 oligofluorene is presented in Scheme 1 and described in the Experimental section (also see Fig. S1 and S2, ESI†). Compound T6 was found to be thermally stable with a decomposition temperature of 436 °C and a glass transition of 106 °C (Fig. S3, ESI†). The photoluminescence (PL) and absorbance spectra of T3, T4 and T6 oligomers in their dilute solutions (in toluene) are shown in Fig. 1b. Fig. S4 (ESI†) also shows the PL and absorbance spectra in solid-films. Photoluminescence spectra of these materials exhibit three vibronic features (0–0, 0–1 and 0–2 transitions) characteristic to these oligofluorenes.[10] In solution, the peak absorbance for T3, T4 and T6 are found at 370, 375 and 379 nm, respectively. As the length of the fluorene arm is increased, both photoluminescence and absorbance features slightly red-shift. This is due to the extension of the π-conjugation in each fluorene arm.[10]

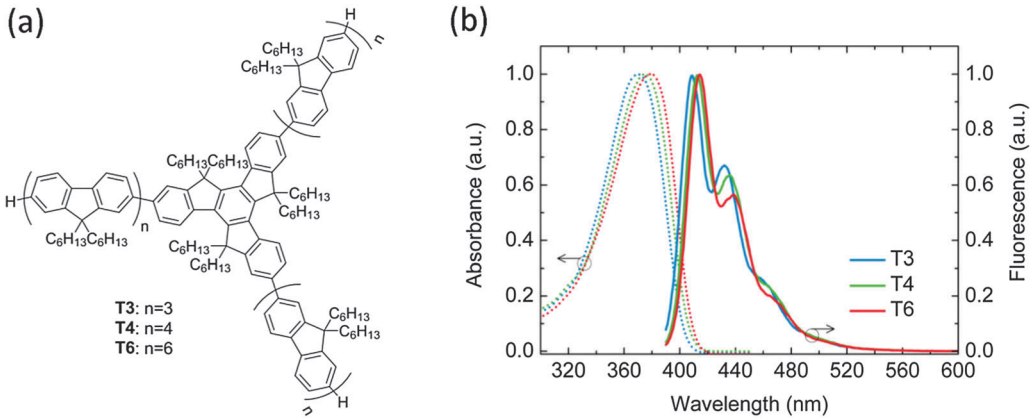

Fig. 1 Molecular structure, emission and absorbance spectra of the star-shaped oligomers with different arm-lengths. (a) Molecular structure of the star-shaped truxene based oligofluorenes having varying fluorene arm lengths. (b) Solution-state absorbance and photoluminescence spectra of the T3, T4 and T6 star-shaped oligofluorenes.

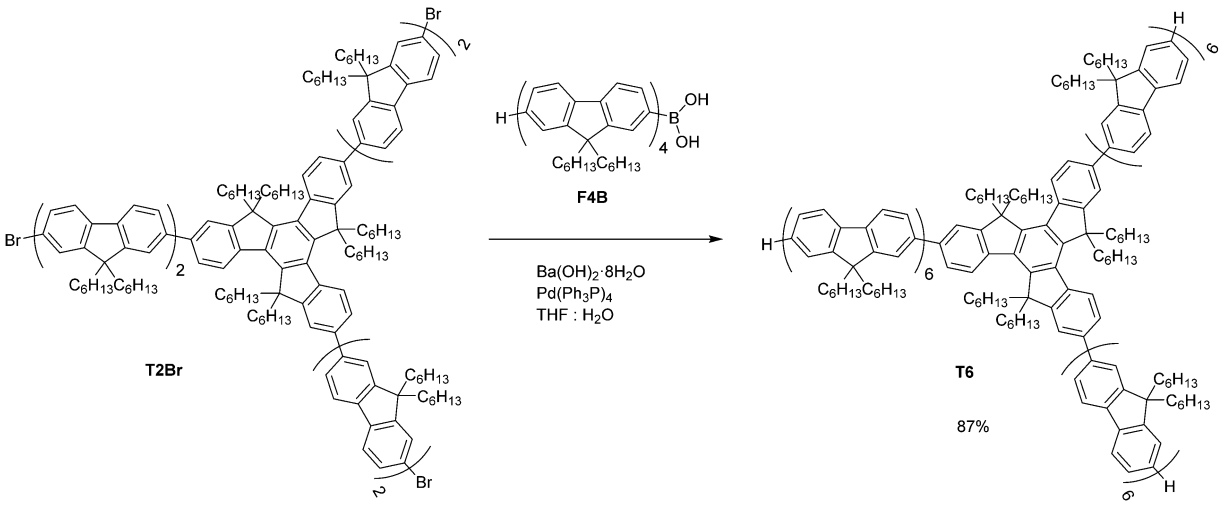

Scheme 1 Synthetic procedure for the T6 compound.

We have previously reported the PL quantum yield in solid-state films of T3 and T4 molecules in the range of 60–86%.[6,8,10,33] In the solid film of T6, we found that the photoluminescence quantum yield was 67% (±5%), which is comparable to that of the T3 and T4 molecules. Previously, we have observed a slight increase in PL quantum yield of oligofluorenes with increasing arm lengths in T1–T4 molecules.[6]

To date, various design strategies have been developed to enhance the nonlinear optical response in organic semiconductors.[29,30] These included developing molecules with central bridge units acting as electron donors or acceptors, branched molecular structures, elongation of π-conjugation and increasing the electronic coupling *via* tailoring of the molecular conformation.[29] Formerly, increasing the number of chromophore units in porphyrin molecules was shown to enhance the 2PA cross-section due to increased delocalization within the molecule.[28,39] Additionally, the increased radial structure of the molecules has been shown to increase the 2PA cross-section too.[15]

We employ a similar design strategy in star-shaped oligofluorenes by increasing the length of the fluorene arms, from three to six fluorene units. Red-shifting of the absorption and photoluminescence features with increasing arm lengths is in accordance with our previous observation with truxene-based oligomers with different arm lengths exhibiting a linear relationship between the red-shift (ΔE) and the reciprocal of the number of benzene rings in the arms of the molecules.[6] Also, this slight red-shift may suggest an extended π-conjugation in these oligomers. Therefore, this is expected to enable enhanced nonlinear optical absorption. Previously, the linear absorption cross-section of the star-shaped oligofluorenes with increasing arm lengths were shown to exhibit up to 3-fold enhancement as compared to their linear oligomer counterparts owing to the branching of the molecular structure.[10]

Here, we investigated the nonlinear optical absorption cross-section *via* the open aperture z-scan technique.[40] The transmittance of a Gaussian laser beam (800 nm, 120 fs, 1 kHz repetition rate and 3.8 μJ per pulse energy) was measured through a 1 mm

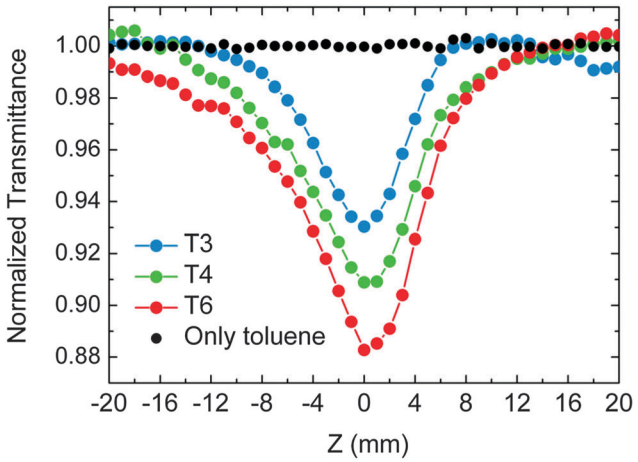

Fig. 2 Open aperture z-scan measurement of the nonlinear absorption cross-section. Normalized transmittance of the Gaussian laser beam (800 nm, 120 fs and 1 kHz repetition rate) through a 1 mm quartz cuvette containing 10 mM of T3, T4, T6 and only toluene, measured by the open aperture z-scan technique.

quartz cuvette containing the oligomer solution (10 mM in toluene) as the sample was translated through the focal plane of the laser beam (a total length of 4 cm). Simultaneously, we monitored the excitation beam intensity during the course of the z-scan measurement using a beam splitter. The transmittance of the laser as a function of the position of the sample on the translational stage is shown in Fig. 2 together with the transmittance of only toluene, in which there is no discernible change in the transmittance signal at the same excitation intensity level. This indicates that the change observed in the transmittance signal is only due to nonlinear absorption in the oligomers. The measured transmittance for three different oligofluorenes (T3, T4 and T6) were fitted using the relation[41]

$$T(z) = \frac{1}{1 + \frac{I_0 \times \beta \times l}{1 + \left(\frac{z}{z_0}\right)^2}} \quad (1)$$

where $T(z)$ is the normalized transmittance as a function of the sample position on z, I_0 is the peak on-axis irradiance at the focus (3.62 W m^{-2}), β is the two-photon absorption coefficient, l is the cuvette length of 1 mm and z_0 is the Rayleigh range ($\sim$3.5 mm). Then, we calculated the 2PA cross section using the following equation

$$\sigma_{2PA} = \frac{h \times \nu \times \beta}{N_A \times d_0 \times 10^{-3}}. \quad (2)$$

Here $h\nu$ is the energy of the excitation photons, N_A is Avagadro's number and d_0 is the molar concentration of the solution (10 mM). The 2PA cross-sections in the T3, T4 and T6 molecules are calculated to be 915, 1628 and 2183 GM (10^{-50} cm^4 s per photon). T6 exhibits the largest 2PA cross-section as compared to T4 and T3. The 2PA cross-section of T6 is comparable to that of blue-emitting conjugated polymers (up to 4000 GM) that are much larger in molecular weight.[20] Also, the 2PA cross-section increases nonlinearly as a function of the number of repeating fluorene units.[39]

We studied the amplified spontaneous emission in these truxene-based oligofluorenes under 2PA pumping (800 nm, 120 fs, and 1 kHz repetition rate). For this purpose, we spin-coated the star-shaped oligofluorenes on pre-cleaned quartz substrates at 1200 rpm for 2 min from solutions having the same molarities (10 mM in toluene). The resulting film thicknesses were measured to be $\sim$300–500 nm using a Dektak profilometer. We used a 20 cm cylindrical lens to focus the laser beam on the sample with a stripe geometry (the area of $\sim$0.11 cm^2 measured using a beam profiler). The PL spectra of the samples were recorded from the edge of the sample *via* a fiber-coupled spectrometer at varying pump intensities (see Fig. 3a for the experimental setup). At low pump intensities, the emission full-width at half-maximum (FWHM) was $\sim$40–50 nm in these oligofluorene samples. As the pump intensity was increased above the ASE threshold, we observed a narrower emission that builds in the deep-blue region ($\sim$430–450 nm) of the spectrum as shown in Fig. 3b–d in the case of T3, T4 and T6 molecules, respectively. The FWHM of the ASE can be as narrow as 5.8 nm, shown by the changing FWHM of the samples in the insets of Fig. 3b–d. Therefore, 2PA pumped ASE is achieved in all these three oligomers.

Fig. 3e shows the pump intensity *vs.* integrated emission intensity under 2PA pumping in these three oligomers. We can clearly see the threshold behavior of an amplified spontaneous emission. The lowest 2PA pumped ASE threshold (2.43 mJ cm^{-2}) is achieved in the T6 molecules. In the T4 and T3 molecules, the 2PA pumped ASE threshold is $\sim$2.80 mJ cm^{-2} for both molecules. Owing to the enhanced 2PA cross-section in T6 molecules, they outperform both T3 and T4 oligomers. Also, the photoluminescence lifetime of the T6 molecules is faster in comparison to that of the T3 and T4 molecules in solid-state films (see Fig. S5, ESI†). Furthermore, we have checked the 1PA ASE performance in T6 molecules (see Fig. S6, ESI†). The 1PA pumped (400 nm, 120 fs, 1 kHz) ASE threshold is as low as 1.43 μJ cm^{-2}. That is much smaller than the previously reported 1PA ASE thresholds in T3 and T4 molecules.[8,42] Yet, the reduced threshold mainly arises from the use of a femtosecond pump laser because previously only nanosecond pump lasers have been employed for 1PA pumping of star-shaped oligofluorenes. It is also worth noting that the position of the ASE peak under 2PA pumping is the same as the 1PA pumped case. This strongly suggests that there is neither degradation nor a heating effect due to 2PA pumping.

The 2PA pumped ASE threshold of 2.43 mJ cm^{-2} obtained in T6 molecules is ultra-low among other types of organic semiconductors. Previously, oligomer based organic crystals and dendrimers could achieve 3.5 and 4.9 mJ cm^{-2} thresholds, respectively.[31,43] To date, only dye-doped polymer based composite media were able to achieve lower 2PA pumped ASE thresholds (1–2 mJ cm^{-2}) than our case, but they suffer from stability issues.[44] Also, colloidal semiconductor nanocrystals, which are alternative competitive materials for 2PA pumped ASE owing to their giant 2PA cross-sections (>20,000 GM), could only offer

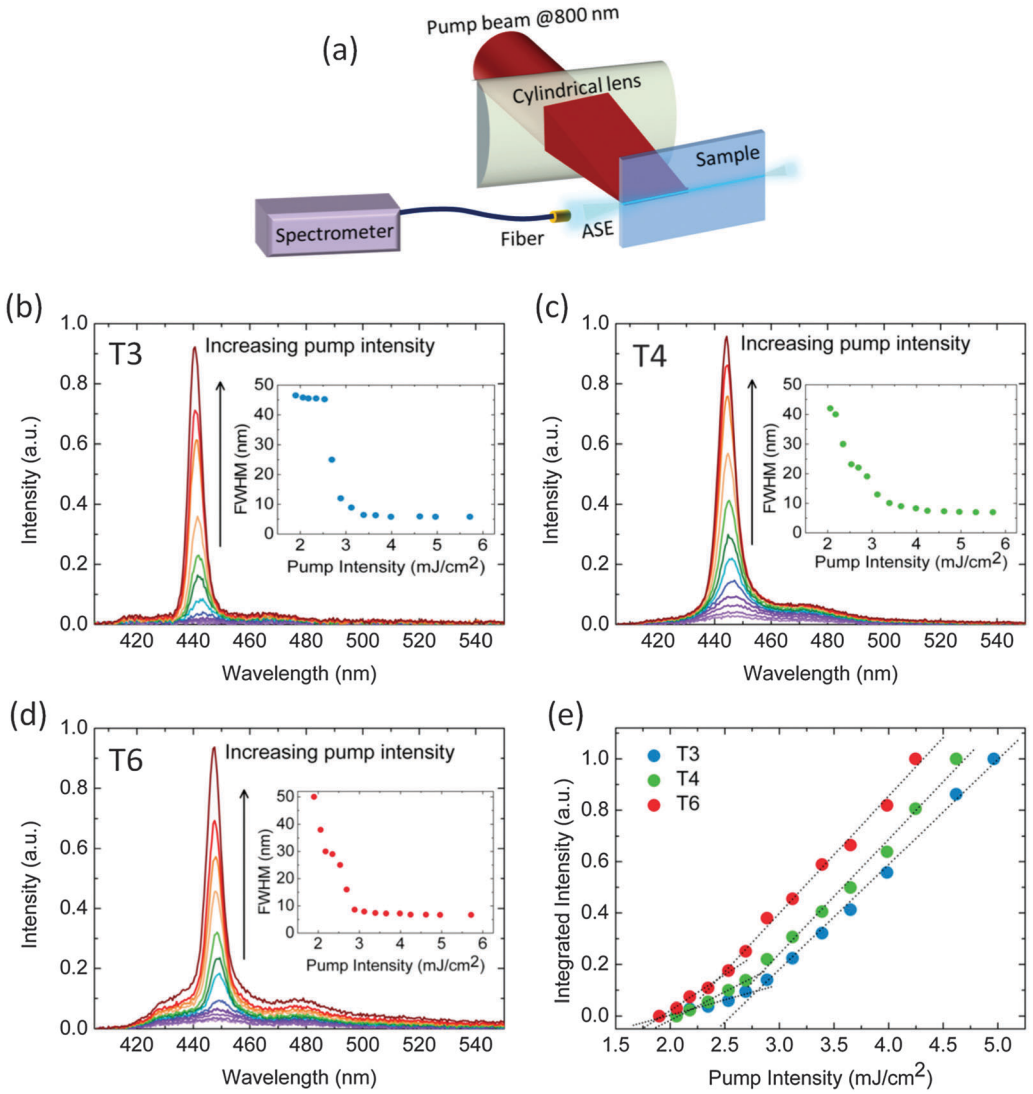

Fig. 3 2PA pumped ASE in the star-shaped oligomers with different arm-lengths. (a) Schematic of the experimental setup for the measurement of the ASE in the spin-coated samples of the oligomers. Two-photon pumped emission and ASE spectra in (b) T3, (c) T4 and (d) T6 molecules as a function of the increasing pump intensity. (b)–(d) The insets show the change of the FWHM emission as a function of the pump intensity. (e) Pump intensity *vs.* integrated emission intensity in T3, T4 and T6 molecules under 2PA pumping clearly exhibiting a threshold behavior.

ASE thresholds on the order of 4–10 mJ cm^{-2} for an ASE in the visible spectral region.[41,45–49] Therefore, star-shaped oligomers with their ultra-low 2PA pumped ASE thresholds while being highly stable under 2PA pumping can serve in various applications as efficient nonlinearly pumped light-emitters.

The observed ultra-low threshold for 2PA pumped ASE in these star-shaped oligofluorenes proves that they are potential candidates as optical gain media in frequency up-converted lasers. To this end, we developed, for the first time, a frequency up-converted laser of the star-shaped T6 oligofluorene using a flexible polymeric distributed feedback (DFB) grating. The flexible DFB gratings were fabricated by copying from a master grating to a 1,4-cyclohexyldimethanol divinyl ether (CHDV) polymer that is hardened under UV light.[11] The resonance wavelength of this two-dimensional grating is calculated using $\lambda_{Bragg} = 2n_{eff}\Lambda/m$, where n_{eff} is the effective refractive index of the laser gain medium, Λ is the period of the two-dimensional grating and m is the Bragg order. Here, we chose the period of the grating to be 266 nm, which matches the resonance wavelength in the 420–460 nm range when m is equal to 2. Therefore, the emission of the laser is perpendicular to the plane of the grating structure (see Fig. 4a).

On top of the flexible DFB structure, we spin-coated T6 molecules (30 mg mL^{-1}) giving a thickness of $\sim$500 $\pm$ 20 nm. The effective refractive index of the laser medium was found to be $\sim$1.65 and the refractive index of the star-shaped oligofluorenes was previously measured to be $\sim$1.77.[6,8] The lasing action was first investigated under 1PA pumping. Here, we employed a spherical lens (20 cm) to focus the pump beam (400 nm, 120 fs, 1 kHz) on the sample with an area of 0.006 cm^2. The emission

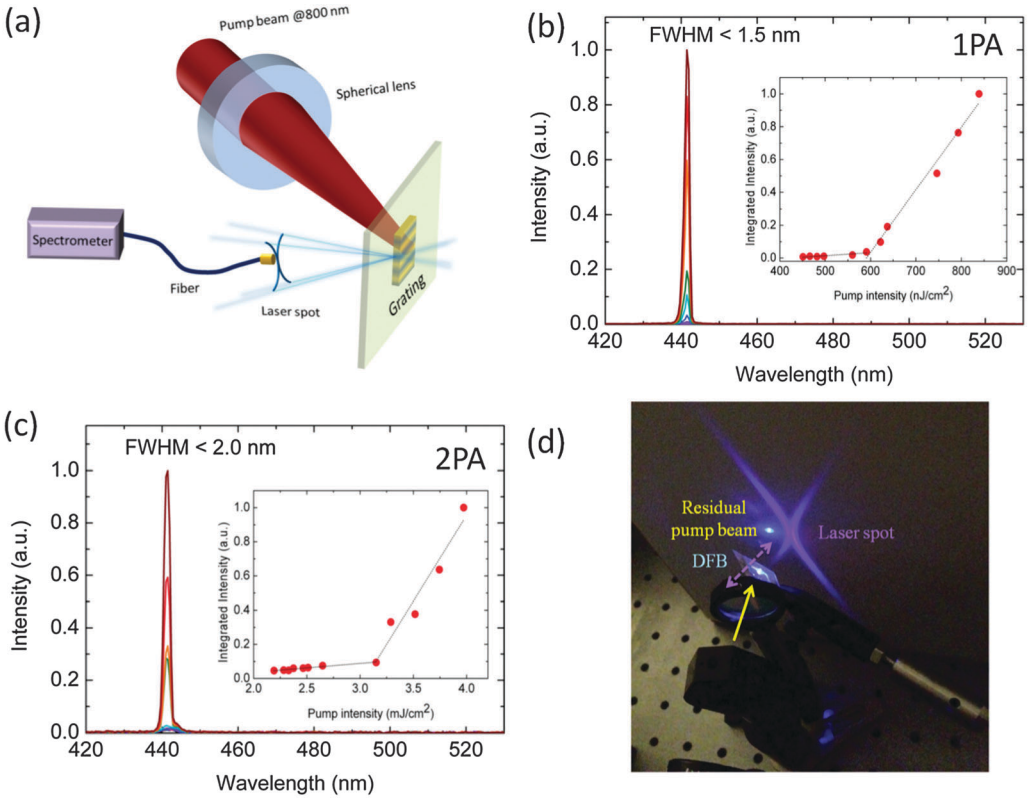

Fig. 4 1PA and 2PA pumped laser of the T6 molecules. (a) Schematic of the experimental setup for the characterization of the frequency up-converted laser of the T6 oligomer. The flexible DFB laser of the T6 oligomer under (b) 1PA pumping and (c) 2PA pumping. (b) and (c) The insets show the pump intensity *vs.* integrated emission intensity from the laser exhibiting the lasing thresholds. (d) Photograph of the frequency up-converted laser of T6 showing the fan-shaped laser beam on the screen.

spectra from the sample at increasing pump intensities are shown in Fig. 4b. The laser has a peak emission at 441 nm with a FWHM less than 1.5 nm limited by the resolution of our spectrometer (Maya 2000). The threshold behavior is demonstrated by the pump intensity *vs.* integrated emission intensity measurement as shown in the inset of Fig. 4b. The 1PA pumped threshold of the T6 based DFB laser is 600 nJ cm^{-2}, which is ultra-low in organic semiconductors. The achieved 1PA pumped lasing threshold is better than that of the other types of oligomers ($\sim$1 μJ cm^{-2})[50] and starburst macromolecular organic semiconductors ($\sim$3 μJ cm^{-2}).[9] Also, our 1PA pumped laser threshold is comparable to that (300 nJ cm^{-2}) of the pyrene-cored oligomer based lasers.[51] Previously, 1PA pumped lasing was studied in both star-shaped T3 and T4 oligofluorenes[8,11] but the lasing thresholds were reported to be relatively large ($\sim$2.7 μJ cm^{-2}). This was due to the use of nanosecond pump lasers.

Next, we demonstrated frequency up-converted lasing in the star-shaped oligomers using the same DFB sample, where the T6 molecules were deposited on top of the 2D grating. The 2PA pumping conditions were the same as those described in the 2PA pumped ASE experiments, except that this time the pump beam (800 nm, 120 fs, 1 kHz) was focused by a spherical lens (f = 20 cm) to an area of 0.022 cm^2. Fig. 4c shows the emission spectra of the frequency up-converted DFB laser as the two-photon pump intensity is gradually increased. The emission peak of the laser was 441 nm, the same as in the 1PA pumping case. The FWHM of the lasing peak is 1.6 nm. The inset in Fig. 4c reveals the pump intensity *vs.* integrated emission intensity, where the 2PA pumped lasing threshold is found to be as low as 3.1 mJ cm^{-2}. The lasing threshold is slightly larger than the threshold (2.43 mJ cm^{-2}) of the 2PA pumped ASE. This is attributed to the fact that the flexible grating material was also absorbing 800 nm femtosecond pulses at intensity levels close to the lasing threshold; thus, the flexible polymeric material of the grating was starting to degrade during the laser operation. We did not observe this in 2PA pumped ASE experiments, since we employed quartz substrates in those cases. The stability of the frequency up-converted laser was found to be limited by $\sim$1–2 $\times$ 10^4 pulses. Yet, the stability of this frequency up-converted laser could be substantially increased by using other substrates for grating such as quartz. Also, we performed all of the lasing experiments under ambient air and did not use any protecting layers to block oxygen or moisture as reported in previous studies.[20,21,31] Fig. 4d shows a photograph of the strong output beam from our frequency up-converted laser, exhibiting a fan-shaped[11] laser beam on a screen together with the residual pump beam. Nevertheless, the achieved frequency up-converter laser threshold (3.1 mJ cm^{-2}) is ultra-low in the literature of organic semiconductors. To date,

there have been several reports that reported thresholds at least an order of magnitude higher than ours including frequency up-converted lasers based on conjugated PFO (42 mJ cm^{-2})[21] and MeLPPP (>200 mJ cm^{-2}) polymers.[20] Recently, Fang *et al.* reported a threshold of 150 μJ cm^{-2} using small organic molecules, where this threshold is calculated specifically based on the absorbed energy (generally 3% of the total incident energy)[21] by the active gain medium.[32] Therefore, their 2PA pumped laser threshold would be expected to be 4–5 mJ cm^{-2}. To the best of our knowledge, our achievement of 3.1 mJ cm^{-2} threshold for frequency up-converted organic semiconductor lasers is the lowest with similar experimental conditions (*i.e.*, pulse duration, repetition rate, excitation geometry and spot size) as compared to the previous reports (see Table S1, ESI†). Furthermore, the laser output is highly polarized due to the 1D DFB structure.[52–54]

Conclusions

In conclusion, we synthesized for the first time the star-shaped oligofluorene T6 molecules having six fluorene repeating units in each arm of the molecule for simultaneously achieving a large 2PA cross-section, large oscillator strength and high PL quantum yield. The resulting T6 oligofluorenes exhibit substantially enhanced nonlinear absorption owing to the elongated π-conjugation and the radial structure in the molecule. The two-photon absorption pumped ASE performance of the T6 oligomers exhibited a lower threshold as compared to that of the T3 and T4 molecules having three and four fluorene units in each arm of the oligomer. The T6 oligomers achieve the best 2PA pumped ASE threshold (~2.43 mJ cm^{-2}) in the organic semiconductors. Also, we show here the first frequency up-converted laser using star-shaped oligofluorenes exhibiting a surpassing performance better than those of all other conjugated polymers. Therefore, these achievements suggest that star-shaped oligomers are the most promising candidates for nonlinearly pumped light-emitting materials. Their frequency up-converted lasers in the deep-blue region pumped by relatively low intensity NIR lasers make them highly attractive for many applications such as photodynamic therapy and bio-sensing.

Acknowledgements

The authors would like to thank the following funding agencies for financial support: EU-FP7 Nanophotonics4Energy NoE, and TUBITAK EEEAG 109E002, 109E004, 110E010, 110E217, 112E183, and 114E410, ESF-EURYI, TUBA-GEBIP and in part from Singapore National Research Foundation under the programs of NRF-RF-2009-09, NRF-CRP-6-2010-02, the Science and Engineering Research Council, Agency for Science, Technology and Research (A*STAR) of Singapore (Project Nos. 092 101 0057 and 112 120 2009) and EPSRC (EP/I029141). H. V. D. acknowledges support from ESF-EURYI and TUBA-GEBIP. P. J. S. thanks the Royal Society for a Wolfson Research Merit Award.

References

1 N. Tessler, G. J. Denton and R. H. Friend, *Nature*, 1996, **382**, 695–697.
2 M. D. McGehee and A. J. Heeger, *Adv. Mater.*, 2000, **12**, 1655–1668.
3 I. D. W. Samuel and G. A. Turnbull, *Chem. Rev.*, 2007, **107**, 1272–1295.
4 S. Chénais and S. Forget, *J. Soc. Chem. Ind.*, 2011, **61**, 390–406.
5 A. L. Kanibolotsky, I. F. Perepichka and P. J. Skabara, *Chem. Soc. Rev.*, 2010, **39**, 2695–2728.
6 A. L. Kanibolotsky, R. Berridge, P. J. Skabara, I. F. Perepichka, D. D. C. Bradley and M. Koeberg, *J. Am. Chem. Soc.*, 2004, **126**, 13695–13702.
7 J. Pei, J.-L. Wang, X.-Y. Cao, X.-H. Zhou and W.-B. Zhang, *J. Am. Chem. Soc.*, 2003, **125**, 9944–9945.
8 G. Tsiminis, Y. Wang, P. E. Shaw, A. L. Kanibolotsky, I. F. Perepichka, M. D. Dawson, P. J. Skabara, G. A. Turnbull and I. D. W. Samuel, *Appl. Phys. Lett.*, 2009, **94**, 243304.
9 W.-Y. Lai, R. Xia, Q.-Y. He, P. A. Levermore, W. Huang and D. D. C. Bradley, *Adv. Mater.*, 2009, **21**, 355–360.
10 N. A. Montgomery, J.-C. Denis, S. Schumacher, A. Ruseckas, P. J. Skabara, A. Kanibolotsky, M. J. Paterson, I. Galbraith, G. A. Turnbull and I. D. W. Samuel, *J. Phys. Chem. A*, 2011, **115**, 2913–2919.
11 J. Herrnsdorf, B. Guilhabert, Y. Chen, A. Kanibolotsky, A. Mackintosh, R. Pethrick, P. Skabara, E. Gu, N. Laurand and M. Dawson, *Opt. Express*, 2010, **18**, 25535–25545.
12 K. Kreger, M. Bäte, C. Neuber, H.-W. Schmidt and P. Strohriegl, *Adv. Funct. Mater.*, 2007, **17**, 3456–3461.
13 W. R. Zipfel, R. M. Williams and W. W. Webb, *Nat. Biotechnol.*, 2003, **21**, 1369–1377.
14 D. R. Larson, W. R. Zipfel, R. M. Williams, S. W. Clark, M. P. Bruchez, F. W. Wise and W. W. Webb, *Science*, 2003, **300**, 1434–1436.
15 M. Albota, *Science*, 1998, **281**, 1653–1656.
16 S. Kim, T. Y. Ohulchanskyy, H. E. Pudavar, R. K. Pandey and P. N. Prasad, *J. Am. Chem. Soc.*, 2007, **129**, 2669–2675.
17 I. Polyzos, G. Tsigaridas, M. Fakis, V. Giannetas, P. Persephonis and J. Mikroyannidis, *Chem. Phys. Lett.*, 2003, **369**, 264–268.
18 S. Kawata, H. B. Sun, T. Tanaka and K. Takada, *Nature*, 2001, **412**, 697–698.
19 P.-A. Bouit, G. Wetzel, G. Berginc, B. Loiseaux, L. Toupet, P. Feneyrou, Y. Bretonnière, K. Kamada, O. Maury and C. Andraud, *Chem. Mater.*, 2007, **19**, 5325–5335.
20 C. Bauer, B. Schnabel, E.-B. Kley, U. Scherf, H. Giessen and R. F. Mahrt, *Adv. Mater.*, 2002, **14**, 673–676.
21 G. Tsiminis, A. Ruseckas, I. D. W. Samuel and G. a. Turnbull, *Appl. Phys. Lett.*, 2009, **94**, 253304.
22 A. Abbotto, L. Beverina, R. Bozio, S. Bradamante, C. Ferrante, G. A. Pagani and R. Signorini, *Adv. Mater.*, 2000, **12**, 1963–1967.
23 M. Drobizhev, Y. Stepanenko, Y. Dzenis, A. Karotki, A. Rebane, P. N. Taylor and H. L. Anderson, *J. Am. Chem. Soc.*, 2004, **126**, 15352–15353.

24 M.-C. Yoon, S. B. Noh, A. Tsuda, Y. Nakamura, A. Osuka and D. Kim, *J. Am. Chem. Soc.*, 2007, **129**, 10080–10081.
25 M. Williams-Harry, A. Bhaskar, G. Ramakrishna, T. Goodson, M. Imamura, A. Mawatari, K. Nakao, H. Enozawa, T. Nishinaga and M. Iyoda, *J. Am. Chem. Soc.*, 2008, **130**, 3252–3253.
26 P. Hrobárik, V. Hrobáriková, I. Sigmundová, P. Zahradník, M. Fakis, I. Polyzos and P. Persephonis, *J. Org. Chem.*, 2011, **76**, 8726–8736.
27 B. R. Cho, K. H. Son, S. H. Lee, Y.-S. Song, Y.-K. Lee, S.-J. Jeon, J. H. Choi, H. Lee and M. Cho, *J. Am. Chem. Soc.*, 2001, **123**, 10039–10045.
28 M. Drobizhev, Y. Stepanenko, A. Rebane, C. J. Wilson, T. E. O. Screen and H. L. Anderson, *J. Am. Chem. Soc.*, 2006, **128**, 12432–12433.
29 M. Pawlicki, H. A. Collins, R. G. Denning and H. L. Anderson, *Angew. Chem., Int. Ed.*, 2009, **48**, 3244–3266.
30 G. S. He, L.-S. Tan, Q. Zheng and P. N. Prasad, *Chem. Rev.*, 2008, **108**, 1245–1330.
31 G. Tsiminis, J.-C. Ribierre, A. Ruseckas, H. S. Barcena, G. J. Richards, G. A. Turnbull, P. L. Burn and I. D. W. Samuel, *Adv. Mater.*, 2008, **20**, 1940–1944.
32 H.-H. Fang, S.-Y. Lu, X.-P. Zhan, J. Feng, Q.-D. Chen, H.-Y. Wang, X.-Y. Liu and H.-B. Sun, *Org. Electron.*, 2013, **14**, 762–767.
33 Y. Wang, G. Tsiminis, Y. Yang, A. Ruseckas, A. L. Kanibolotsky, I. F. Perepichka, P. J. Skabara, G. A. Turnbull and I. D. W. Samuel, *Synth. Met.*, 2010, **160**, 1397–1400.
34 B. Guilhabert, N. Laurand, J. Herrnsdorf, Y. Chen, A. R. Mackintosh, A. L. Kanibolotsky, E. Gu, P. J. Skabara, R. A. Pethrick and M. D. Dawson, *J. Opt.*, 2010, **12**, 035503.
35 K. Shi, J.-Y. Wang and J. Pei, *Chem. Rec.*, 2015, **15**, 52–72.
36 G. Tsiminis, N. A. Montgomery, A. L. Kanibolotsky, A. Ruseckas, I. F. Perepichka, P. J. Skabara, G. A. Turnbull and I. D. W. Samuel, *Semicond. Sci. Technol.*, 2012, **27**, 094005.
37 D. R. Coulson, L. C. Satek and S. O. Grim, in *Inorganic Syntheses*, ed. F. A. Cotton, John Wiley & Sons, Inc, Hoboken, NJ, USA, 2007, pp. 121–124.
38 C. R. Belton, A. L. Kanibolotsky, J. Kirkpatrick, C. Orofino, S. E. T. Elmasly, P. N. Stavrinou, P. J. Skabara and D. D. C. Bradley, *Adv. Funct. Mater.*, 2013, **23**, 2792–2804.
39 M. Drobizhev, A. Karotki, Y. Dzenis, A. Rebane, Z. Suo and C. W. Spangler, *J. Phys. Chem. B*, 2003, **107**, 7540–7543.
40 M. Sheik-Bahae, A. A. Said, T.-H. Wei, D. J. Hagan and E. W. Van Stryland, *IEEE J. Quantum Electron.*, 1990, **26**, 760–769.
41 A. F. Cihan, Y. Kelestemur, B. Guzelturk, O. Yerli, U. Kurum, H. G. Yaglioglu, A. Elmali and H. V. Demir, *J. Phys. Chem. Lett.*, 2013, **4**, 4146–4152.
42 Y. Chen, J. Herrnsdorf, B. Guilhabert, A. L. Kanibolotsky, A. R. Mackintosh, Y. Wang, R. A. Pethrick, E. Gu, G. A. Turnbull and P. J. Skabara, *Org. Electron.*, 2011, **12**, 62–69.
43 H.-H. Fang, Q.-D. Chen, J. Yang, H. Xia, B.-R. Gao, J. Feng, Y.-G. Ma and H.-B. Sun, *J. Phys. Chem. C*, 2010, **114**, 11958–11961.
44 W. Li, C. Zhang, Q. Chen, X. Wang and M. Xiao, *Appl. Phys. Lett.*, 2012, **100**, 133305.
45 Y. Kelestemur, A. F. Cihan, B. Guzelturk and H. V. Demir, *Nanoscale*, 2014, **6**, 8509–8514.
46 B. Guzelturk, Y. Kelestemur, M. Z. Akgul, V. K. Sharma and H. V. Demir, *J. Phys. Chem. Lett.*, 2014, **5**, 2214–2218.
47 B. Guzelturk, Y. Kelestemur, M. Olutas, S. Delikanli and H. V. Demir, *ACS Nano*, 2014, **8**, 6599–6605.
48 B. Guzelturk, Y. Kelestemur, K. Gungor, A. Yeltik, M. Z. Akgul, Y. Wang, R. Chen, C. Dang, H. Sun and H. V. Demir, *Adv. Mater.*, 2015, **27**, 2741–2746.
49 M. Olutas, B. Guzelturk, Y. Kelestemur, A. Yeltik, S. Delikanli and H. V. Demir, *ACS Nano*, 2015, **9**, 5041–5050.
50 Y. Qian, Q. Wei, G. Del Pozo, M. M. Mróz, L. Lüer, S. Casado, J. Cabanillas-Gonzalez, Q. Zhang, L. Xie, R. Xia and W. Huang, *Adv. Mater.*, 2014, **26**, 2937–2942.
51 R. Xia, W.-Y. Lai, P. A. Levermore, W. Huang and D. D. C. Bradley, *Adv. Funct. Mater.*, 2009, **19**, 2844–2850.
52 C. Kallinger, M. Hilmer, A. Haugeneder, M. Perner, W. Spirkl, U. Lemmer, J. Feldmann, U. Scherf, K. Müllen, A. Gombert and V. Wittwer, *Adv. Mater.*, 1998, **10**, 920–923.
53 W. Holzer, A. Penzkofer, T. Pertsch, N. Danz, A. Bräuer, E. B. Kley, H. Tillmann, C. Bader and H.-H. Hörhold, *Appl. Phys. B: Lasers Opt.*, 2002, **74**, 333–342.
54 G. Heliotis, R. Xia, D. D. C. Bradley, G. A. Turnbull, I. D. W. Samuel, P. Andrew and W. L. Barnes, *Appl. Phys. Lett.*, 2003, **83**, 2118.